

On the Capacity of Fractal D2D Social Networks with Hierarchical Communications

Ying Chen, Rongpeng Li, Zhifeng Zhao, and Honggang Zhang

Abstract—The maximum capacity of fractal D2D (device-to-device) social networks with both direct and hierarchical communications is studied in this paper. Specifically, the fractal networks are characterized by the direct social connection and the self-similarity. Firstly, for a fractal D2D social network with direct social communications, it is proved that the maximum capacity is $\Theta\left(\frac{1}{\sqrt{n \log n}}\right)$ if a user communicates with one of his/her direct contacts randomly, where n denotes the total number of users in the network, and it can reach up to $\Theta\left(\frac{1}{\log n}\right)$ if any pair of social contacts with distance d communicate according to the probability in proportion to $d^{-\beta}$. Secondly, since users might get in touch with others without direct social connections through the inter-connected multiple users, the fractal D2D social network with these hierarchical communications is studied as well, and the related capacity is further derived. Our results show that this capacity is mainly affected by the correlation exponent ϵ of the fractal structure. The capacity is reduced in proportional to $\frac{1}{\log n}$ if $2 < \epsilon < 3$, while the reduction coefficient is $\frac{1}{n}$ if $\epsilon > 3$.

Index Terms—Capacity, D2D Social Networks, Fractal Networks, Hierarchical Social Communications, Self-Similarity

I. INTRODUCTION

With the explosive increase of smart devices, social network traffic has witnessed unprecedented growth and imposed huge challenge on traditional content delivery paradigm [1]. Particularly, with the increasing awareness of security and privacy, trust has become a prerequisite for interactions between mobile users [2]. People tend to communicate with trusted persons rather than geographically close ones. That is to say, the social connection exists if and only if two users trust each other to some extent. Depending on whether the two communicating parties have mutual trust or not, social communications in the ever-growing D2D (device-to-device) networks can be divided into two major categories:

- *Direct social communications*: The two end users of communication are mutually trusted and directly linked by a social connection. They are likely to share some kind of intimate relationship, such as families, friends, colleagues and so on.
- *Hierarchical social communications*: The two end users of communication are not mutually trusted and are in-

directly connected through a couple of inter-connected users. Rather than the direct communications, they may prefer to transfer information via the inter-connected and trusted users.

This paper aims to investigate the capacity of a fractal D2D social network. As a whole, a fractal D2D social network refers to a social network where the social connections between users are formed according to the fractal patterns, and the overlaying social communication is implemented by an underlying D2D physical network. Due to the possibly long physical distance between the social communication pair of end users, several nodes in the D2D physical network are needed to play the role of relaying, so as forward the data packets. Taking into account security and privacy, these relay nodes are only responsible for data forwarding via Proximity Services (ProSe) Discovery [3] without storing messages. In addition, specific implementation issues in real world are not the emphases of this work, such as how to design an efficient scheduling algorithm [1], how to stimulate the selfish users to cooperate for social transmissions [4], or how to establish the trust relationship between two users [2].

Generally, on one hand, the underlying D2D propagation network allows users in proximity to establish local links and exchange contents directly instead of obtaining data from the cellular infrastructure [4]. On the other hand, different from some well-known fractal structures with specific geometric shapes as studied in [5], [6], [7], the fractal social networks in this paper are those with general fractal characteristics. Within the framework of complex networks, the general fractal features have been well studied [8], [9], [10] and are mainly determined by the degree correlations in the connectivity of the networks, which can be characterized by some well-established models or distributions like [11], [12], [13]. To be specific, the most vital essence of the general fractal networks studied in this paper is described by the two power-law distributions below:

- *Joint probability distribution $P(k_1, k_2)$* : It captures the possibility to establish a social connection between two users with degree k_1 and k_2 , and the degree in a fractal D2D social network refers to the number of social connections of a user. As the fundamental requirement for the general fractal social networks [11], $P(k_1, k_2)$ can be expressed as:

$$P(k_1, k_2) \propto k_1^{-(\gamma-1)} \cdot k_2^{-\epsilon}, \quad (k_1 > k_2) \quad (1)$$

where γ is the degree distribution exponent, ϵ is the correlation exponent, and the operator \propto denotes the

Y. Chen, R. Li, and H. Zhang are with College of Information Science and Electronic Engineering (ISEE), Zhejiang University. Email: {21631088chen_ying, lirongpeng, honggangzhang}@zju.edu.cn. Z. Zhao is with Zhejiang Lab. Email: zhaozf@zhejianglab.com. Corresponding author: R. Li.

This work was supported in part by National Natural Science Foundation of China (No. 61701439, 61731002), Zhejiang Key Research and Development Plan (No. 2019C01002, 2019C03131), the Project sponsored by Zhejiang Lab (2019LC0AB01), Zhejiang Provincial Natural Science Foundation of China (No. LY20F010016).

proportional relationship between the two sides. This form of expression indicates that k_1 and k_2 are mutually independent.

- *Degree distribution $P(k)$* : Another important characteristic of the general fractal network is known as self-similarity. It has been found that a variety of real complex networks consist of self-repeating patterns on all length scales [14]. Self-similarity of a fractal network requires the degree distribution $P(k)$ of a user to remain invariant when the network grows, namely following the so-called scale-free law. In order to meet this requirement, degree distribution must meet Eq. (2) below [15], [16], [17], [18]:

$$P(k) \propto k^{-\gamma}. \quad (2)$$

In essential, the two power-law distributions above lay the foundations for the capacity analysis of fractal D2D social networks.

In such a social networking scenario as stated above, the rationality of the scenario setting and main novelty of this paper are highlighted as following:

1. The fundamental topological feature, i.e., fractal pattern, is introduced into the maximum capacity analysis in social mobile networks. Recently, we have discovered interesting fractal features in wireless networks [19], and to some extent this encourages us to reflect on the potential impact of fractality on network performance. As one of the most important performance indicators, network capacity has been investigated in various scenarios, such as ad-hoc wireless networks by Gupta and Kumar [20], relay-assisted wireless networks in [21], hybrid wireless networks in [22], etc. Nevertheless, to our best knowledge, except the recent works in [5], [6], most documents, including [23], have made few efforts to incorporate such a vital property (i.e. fractality) into the capacity study of wireless networks, let alone social mobile networks.

2. It is of significance to combine fractal patterns and D2D communications together on the basis that they are both tightly associated with social networks. On one hand, social conceptions are of vital importance to enhance the performance of D2D communications in terms of throughput, spectral efficiency, latency and fairness [24]. For example, efficient device cooperation strategies were developed in D2D communications based on two key social phenomena, namely social trust and social reciprocity in [25]. Considering both spatial and social proximity, novel mechanisms for secure D2D communications in user clusters were presented in [26]. [27] qualitatively analyzed how social properties can be beneficial to D2D communications, and augment D2D communication system by leveraging social networking features. [28] claimed that social-aware cooperations in D2D communication exert considerable influence on its further adoption and can decisively promote network performance. On the other hand, fractal patterns have been paid attention to for its further importance in social networks. For instance, there have been evidences that humans are psychologically motivated to form hierarchies, i.e., one of the essential features of fractal patterns, in social networks due to their core needs for order and man-

agement [29]. Beyond traditional approaches, a fractal view was embedded in [30] to evaluate user importance in social networks. In addition, fractal networks are superior to non-fractal ones in terms of resilience, scalability and robustness [31]. Hence, a fractal social network can recover quickly from unpredictable security attacks because the breakdown of a few nodes does not cause the collapse of the whole network. Consequently, it is meaningful to overlay a fractal social network on top of a D2D physical network.

3. It is widely recognized that not only direct social communications but also hierarchical social communications ubiquitously exist in all kinds of social networks. In practical social scenarios, people without mutual familiarity do have to communicate with each other from time to time. Nevertheless, in regard to security and privacy, people may prefer to transfer critical information via the inter-connected, familiar and trusted users. What's more, hierarchical social communications involve more intermediate relay users than direct social communications, thus causing longer transmission path needing some kind of delay tolerance in the social sense. Therefore, the fractal topology of social networks has a greater impact on the capacity in hierarchical case, which is consistent with our study purpose.

A. Related Works

As a key component of future 5G mobile networks to improve throughput and spectral efficiency, D2D communication has been investigated in many contexts. Particularly, a number of literatures concerning with the D2D social networks have sprung up. For instance, [32] analyzed the performance of relay-assisted multi-hop D2D communication where the decision to relay was made based on social comparison. In order to alleviate the security issue in D2D social networks, a secure content sharing protocol was proposed in [33] to meet the security requirements. In regard to the significance of trust and social-aware cooperation between end users and network operators for the widespread adoption of the direct communications paradigm, [28] advanced the vision of social-aware and trusted D2D connectivity. To achieve successful content uploading services by user cooperation in D2D communication despite malicious nodes, reliability and reputation notions are considered to model the level of trust among the involved users [34]. Essentially, these works are related and complementary to this paper, and they can be integrated eventually. Beyond these existed results, investigations on network capacity can be further expected. Moreover, our work provides another perspective for the research on security mechanism in social networks. In addition, since fractal patterns can be utilized to improve the security level as well, it can be integrated with the results in the existed works to further enhance the security mechanism in social networks.

Moreover, DTNs (delay tolerant networks) and D2D communications share essential similarities by allowing users in proximity to communicate with each other directly. Even so, DTN does possess some unique characteristics in regard to the network setting. A typical DTN generally consists of a sparse set of fixed or mobile nodes [35], and is often characterized

by intermittent connectivity and frequent network partitioning [35]. In DTNs, mobile nodes can only opportunistically exchange messages when they are in the transmission range of each other during a period of time, and a path between a pair of end users can not be guaranteed in any case [36]. Nevertheless, the versatility of D2D communications has led to consideration of its cooperation with IoT (Things of Internet) [37], where the advantage is to provide continuous connectivity (instead of intermittent connectivity) via short-range communications so that service continuity can be guaranteed [38]. Therefore, the network setting for D2D considered in this paper has no strict constraints on the sparse node density, and the continuity in connectivity is feasible to be assumed here. To be specific, two users whose physical distance is under a certain threshold in D2D communications are able to establish stable local links and exchange contents directly under tolerable channel conditions [4], the end-to-end communication exists between any pair of social users with the aid of relaying users via D2D as long as they are physically close enough. One of the benefits from this assumption, D2D leads to tractable mathematical models for capacity analyses, and produces analytical results in closed-forms. However, the stochastic way of space and moving nodes in DTNs might result in the lack of continuous connectivity and possibly unstable network topology [39]. Therefore, plenty of efforts have been made to design applicable routing protocols for DTNs [40], [41], [42], [43], [44]. Unfortunately, most of the existing works need to estimate the probability of two nodes having contact and the time when such contact emerges. If there is no connection available at a particular time, a DTN node can store and carry the data until it encounters other nodes. Thus it can be seen that the complicated and unpredictable nature of DTNs makes it relatively difficult to come up with a straightforward routing strategy.

Actually, DTNs have recently attracted a lot of attention from the research community. For example, in order to analyze the capacity scaling properties in mobile ad-hoc networks with heterogeneous nodes and spatial inhomogeneities, a general framework was provided and proven effective in [35]. Due to the deficiency of the assumption that a node can immediately discover the nodes that move into its transmission range, [36] investigated the impact of contact-probing mechanisms on link duration and, thus the transmission capacity of DTNs. Considering a cell-partitioned model, [45] studied two quantities of interest in a DTN, namely the network capacity region and the minimum energy function.

Among the literatures with regard to D2D social networks, the issue of capacity has barely been considered to our best knowledge. Even so, owing to its fundamental significance, there have existed a great deal of researches on the capacity of various kinds of wireless networks. Philippe Jacquet *et al.* studied the capacity of wireless networks under three models when the emitters and the access point are randomly distributed in an infinite fractal map [5], [6]. Gupta and Kumar firstly proved that the throughput in ad-hoc wireless networks can reach $\Theta\left(\frac{1}{\sqrt{n \log n}}\right)$ when the network size is n [20], where the symbol Θ refers to the order of magnitude. The capacity of

wireless networks under the relay case was studied in [21], and the research on the capacity of hybrid wireless networks was conducted in [22]. Kulkarni *et al.* provided a very elementary deterministic approach on the capacity of wireless networks, which gave throughput results in terms of the node locations [46]. For social wireless networks, Sadjadpour *et al.* studied the capacity of a scale-free wireless network in which nodes communicate with each other in the context of social groups [47]. Particularly, it was discovered that the maximum capacity can be improved in the social scale-free networks compared with the classical conclusion drawn by Gupta and Kumar [23], [48]. In addition, they studied the capacity of composite networks, namely, the combination of social and wireless ad-hoc networks [49]. Bitar Azimdoost *et al.* investigated the capacity and latency in an information-centric network when the data cached in each node has a limited lifetime [50].

In spite of the fact that a vast amount of documents have studied the capacity of various wireless networks, the capacity of fractal networks has been paid little attention to. However, as a vital property of networks, fractal phenomenon has already been discovered in many wireless networking scenarios [19]. For example, the coverage boundary of the wireless cellular networks shows a fractal shape, and the fractal features can inspire the new design of the hand-off scheme in mobile terminals [51], [52]. Moreover, a large number of significant networks in the real world exhibit the fractal characteristics naturally, such as the world-wide web, yeast interaction, protein homology, and social networks [14], [53]. In addition, the concept of fractal structure has been taken advantage of in various applications, including the design of antennas for satellite down-link and up-link communications, wireless local area network (WLAN) applications, and other 5G applications [54], [55].

In summary, as one potentially groundbreaking work, this paper studies the capacity of fractal D2D social networks.

B. Contribution

Distinct from the previous works, the maximum capacity of fractal D2D social networks with both direct and hierarchical interconnections among the users is addressed in this paper. In this regard, some key novel contributions are provided as following:

- First of all, the capacity of fractal D2D social networks with direct social communications is elaborated. On one hand, it is proven that if a user communicates with one of his/her direct contacts in a random manner, the maximum capacity is $\Theta\left(\frac{1}{\sqrt{n \log n}}\right)$. On the other hand, if the two users with inter-distance d communicate according to the probability in proportion to $d^{-\beta}$, the maximum capacity can reach up to $\Theta\left(\frac{1}{\log n}\right)$.
- Secondly, the relationship between the extendibility of a fractal social network and the correlation exponent ϵ is revealed according to the definition in Eq. (1) and Eq. (2). It is mathematically proven that $\epsilon=3$ is the boundary to distinguish whether a fractal network is extensible or not. The fractal network can expand branches continuously

when $2 < \epsilon \leq 3$, while the fractal network stops branching rapidly if $\epsilon > 3$.

- Thirdly, the capacity of fractal D2D social networks with hierarchical communications is derived. Compared to the results with direct social communications, it turns out that: 1) If $2 < \epsilon < 3$, the order of the capacity decreases in proportion to $\frac{1}{\log n}$; 2) If $\epsilon = 3$, the capacity reduces in proportion to $\frac{1}{n}$, which reflects the trade-off between the security and capacity of fractal D2D social networks.

Actually, the results of our work can be applied to a plenty of networking scenarios. Here are some of the typical examples. In D2D communication, [56] proposed a capacity oriented resource allocation algorithm, which allows a D2D pair to share more than one mobile user's resources to achieve high system capacity. Based on our interesting findings, i.e., the fractal features tend to cut down the capacity of the networks, the resource allocation algorithm can be optimized by arranging the topology appropriately to reduce the fractality of the resource-sharing D2D users' group. Moreover, [57] claimed that the network capacity can be enhanced by increasing the density of D2D users, whilst our findings can provide an additional perspective for [57] by taking into account the topology of D2D network. In social networks, [58] showed that traffic distribution and network capacity can be analyzed by representing a social network as a human contact graph, and further works can be done by characterizing the graph as a fractal network.

The remainder of this paper is organized as follows. The fundamentals of a fractal network as well as the basic knowledge of both direct and hierarchical social communications in fractal D2D networks are introduced, and the corresponding network model is discussed in Section II. Then the maximum throughput with direct social communications is derived in Section III. Afterwards, the deductions are extended to the case with hierarchical social communications in Section IV. Numerical simulation results are discussed in Section V. Finally, a conclusion is drawn in Section VI.

II. BACKGROUND AND MODELS

A. Fundamentals of a Fractal Network

Besides the basic description of a fractal network via the power-law distributions, one of the most popular alternative definition frameworks is based on the concept of renormalization through the box-covering algorithm [12], [13], [14]. Compared with the mathematical power-law distribution method, box-covering algorithm is more explicit and vivid, so it is helpful to introduce the concept of renormalization through the box-covering algorithm to reinforce the understanding of fractal features.

As illustrated in Fig. 1, renormalization is a technique to examine the internal relationship among the nodes in a complex network by using a box to cover several nodes and virtually replacing the whole box by a new representative node. Besides, if there exists a link between any two nodes in two boxes respectively, then the two corresponding representative nodes evolved from the boxes will be connected.

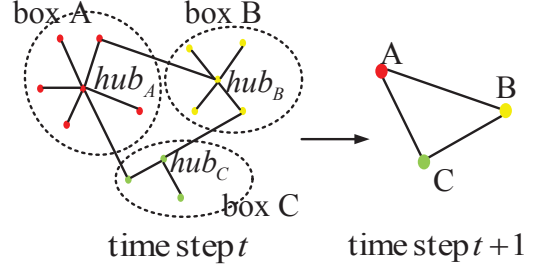


Fig. 1: The illustration of renormalization of a fractal network.

Mathematically, the network can be minimally covered by $N_B(l_B)$ boxes of the same length scale l_B under renormalization, where l_B is the size of the box measured by the maximum path length between any pair of nodes inside the box, and $N_B(l_B)$ is the minimum value among all possible situations. To be specific, the size of boxes l_B in Fig. 1 is 2 and the number of boxes $N_B(l_B)$ is 3 (box A, B, and C).

In essential, if the network is a general fractal network, the following relations hold, namely [12], [59]:

$$\begin{cases} N_B(l_B)/n \propto l_B^{-d_B} \\ k_B(l_B)/k_{hub} \propto l_B^{-d_g} \\ n_h(l_B)/k_B(l_B) \propto l_B^{-d_e}, \end{cases} \quad (3)$$

where n is the number of nodes in the network. A hub indicates the node with the largest degree inside each box, while $k_B(l_B)$ and k_{hub} denote the degree of the box and the hub respectively. $n_h(l_B)$ refers to the number of links between the hub of a box and the nodes in other connected boxes. Take box A in Fig. 1 for example, the variables $k_B(l_B)$, k_{hub} and $n_h(l_B)$ are 2, 6 and 1, respectively. The three indexes d_g , d_B and d_e indicate the degree exponent, the fractal exponent, and the anti-correlation exponent, respectively.

Viewing the above process of renormalization from the perspective of time steps, the number of boxes $N_B(l_B)$ in this time step is also the number of nodes in the next time step, and the first equation in Eq. (3) indicates that the ratio of the numbers of nodes between successive time steps is proportional to $l_B^{-d_B}$, and the power-law relationship remains unchanged under renormalization, obeying the scale-free law. In a similar way, the degree of the box $k_B(l_B)$ at present is the degree of the hub k_{hub} in the next time step as well, and the second equation in Eq. (3) shows that the ratio of the hub degrees between successive time steps is a scale-invariantly exponential function of the box size l_B . Therefore, what the first and second equations in Eq. (3) reveal is actually the topological self-similarity of fractal networks [12]. In addition, the degree exponent d_g and the fractal exponent d_B are both finite for fractal networks.

Moreover, the ratio $n_h(l_B)/k_B(l_B)$ in the third equation in Eq. (3) reveals the contribution of hub nodes in box-box connections, and it decreases sharply with the increase of the length scale l_B . Actually, this equation illustrates the hub repulsion phenomenon, i.e., a node with a large degree prefers not to be linked to another node with a large degree, which

is another essential property of fractal networks. Therefore, the anti-correlation exponent d_e reveals the repulsion effect between the hubs, and large d_e tends to result in a fractal networking structure. As shown in Fig. 1, instead of establishing a connection with another hub, each hub node prefers to connect with a non-hub node in another box.

In [11], it has been proven that there exist certain relations among the aforementioned key parameters: $\gamma = 1 + \frac{d_B}{d_g}$ and $\epsilon = 2 + \frac{d_e}{d_g}$, which suggest that γ and ϵ in a fractal wireless network are larger than 1 and 2, respectively. Please note that for concision, hereinafter all the following relevant mathematic deductions will be characterized by the key parameters γ and ϵ , instead of d_B , d_g and d_e .

B. Knowledge of Both Direct and Hierarchical Social Communications in Fractal D2D Social Networks

Fig. 2(a) illustrates the direct/*level-1* social communications in a fractal D2D social network. As we can see, four users, namely Bob, Jane, Joy and Rose, are directly connected with Alice and are regarded as the direct, or *level-1* contacts of Alice. If Alice chooses to communicate with Bob among her four direct contacts, then Alice and Bob are known as the source user and the destination user, respectively. Usually, a user has more than one direct contacts, and the degree k refers to the number of his/her *level-1* contacts. In the case of *level-1* social communications, the degree distribution and the joint probability distribution are the aforementioned $P(k)$ and $P(k_1, k_2)$, respectively. As discussed later in Section II-C, the direct/*level-1* contact does not imply there physically exist some direct links. Instead, the pair of users for direct social contact might have to rely on some relay nodes in the underlying physical propagation network.

In addition to the direct case, the social communications in fractal D2D social networks can actually be hierarchical as depicted in Fig. 2(b). If Alice wants to get in touch with Victoria who she does not trust, the data packets have to be transmitted through the inter-users Bob and Jack. That is to say, a source user can communicate with one of his/her *level-L* ($L = 1, 2, \dots, L_{max}$) contacts through $L - 1$ inter-users to make sure that every transmission is carried out between two users with mutual trust, and L_{max} refers to the maximum social relationship level. For instance, in the case of *level-2* social communications, Jack is indirectly connected with the source user Alice through one inter-user Bob, so Jack is one of the *level-2* contacts of Alice, and he can be selected as the destination user among all the *level-2* contacts to communicate with Alice. Similarly, Victoria is referred to as one of the *level-3* contacts of Alice, and so on.

To enhance the understanding of mathematical derivations in Section IV, it is necessary to introduce the concept of *level-L* graphs of the social topology. Without loss of generality, the superscript L is used to denote a *level-L* case. If all *level-2* contact pairs in Fig. 3(a) are connected virtually, then a new graph is obtained as shown in Fig. 3(b). In *level-2* graph, the degree distribution is defined as $P(k^{(2)})$, where the degree $k^{(2)}$ of a user is the *level-2* degree, and refers to the number of his/her *level-2* contacts or his/her links in the *level-2* graph.

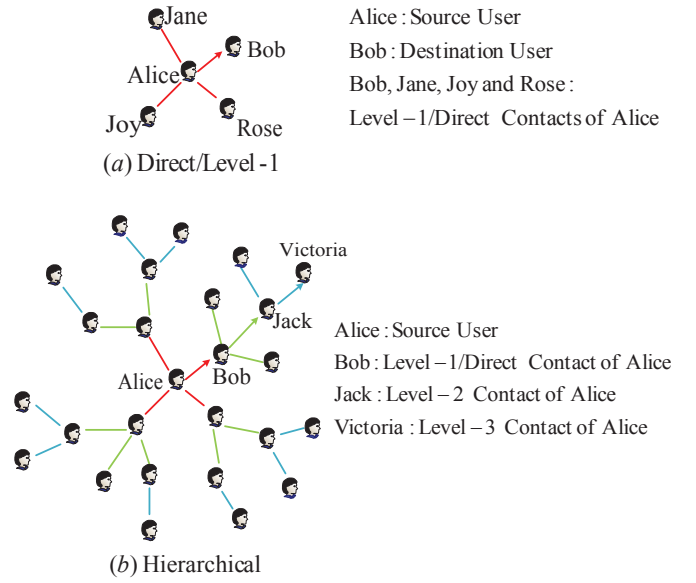


Fig. 2: (a) Direct/*Level-1* social communications in a fractal D2D social network; (b) Hierarchical social communications in a fractal D2D social network.

In the same way, the *level-3* graph can be obtained in Fig. 3(c) by connecting all *level-3* contact pairs virtually, and the degree distribution here is defined as $P(k^{(3)})$, where the degree $k^{(3)}$ of a user is the *level-3* degree, and so forth.

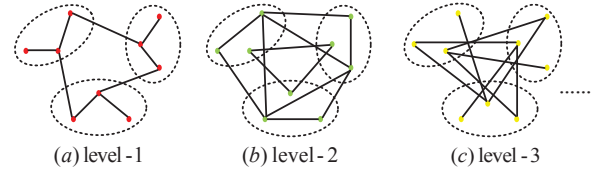


Fig. 3: The *level-L* graphs of the social topology by connecting all *level-L* contact pairs virtually.

C. Network Model

In order to clarify the capacity of the above fractal D2D social networks with both direct and hierarchical communications clearly and orderly, it is assumed that all the n users are uniformly distributed in a unit area square. Also the fractal D2D social network is treated as a static network because the users barely move during one transmission frame.

All the potential users form an underlying D2D propagation network on the physical layer, as well as an overlaying fractal social network from the viewpoint of social connections. An illustrative part of the overlaying fractal D2D social network is shown in Fig. 4(a), and the connection between two users stands for the relationship of mutual trust. It is noteworthy that the topological fractal social network is formed by the D2D social connections of all the involved users following the aforementioned degree distributions $P(k)$ and $P(k_1, k_2)$, which is not contradictory with the general assumption of physically uniformly distributed users as potential relay nodes.

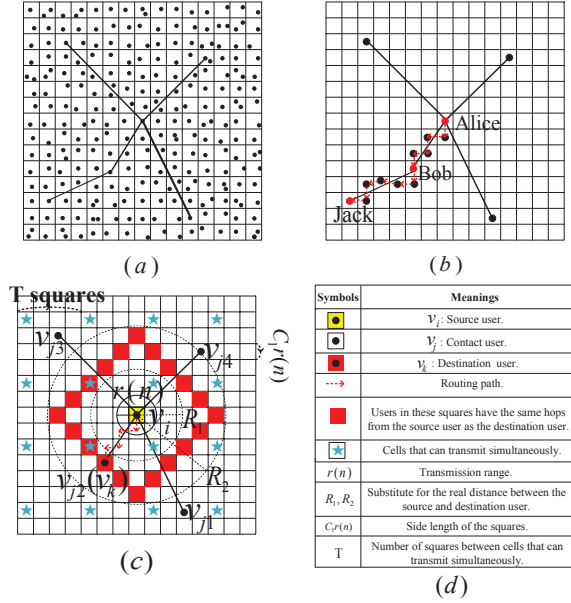


Fig. 4: (a) An illustrative part of the overlaying fractal D2D network with social interconnections; (b) The underlying physical propagation network serves to forward data for a transmission via multi-hop routing between any pair of social contacts; (c) The fractal D2D social network deployed in a standard unit area square model [46], [23]; (d) The table of the symbols in the model.

As depicted in Fig. 4(b), the underlying D2D physical propagation network has to be distinguished from the overlaying fractal social network, where the propagation network serves the social communications and forwards data for a transmission via multi-hop routing between any pair of social contacts. For example, when Alice wants to communicate with Jack, she has to get in touch with Jack through Bob, as we discussed in Section II-B. However, Alice and Bob cannot exchange data directly even though they are socially connected because they are not physically close enough to exchange contents locally. In order to transmit a packet from Alice to Bob, a few other nodes within the underlying D2D propagation network have to serve as relay nodes as the red dotted path in Fig. 4(b) shows, so does the transmission from Bob to Jack. It has been explained in [23] that the relay nodes will never cause traffic bottleneck, so the underlying propagation network will not change the capacity of the overlaying social network. Please note that this kind of multi-hop data relaying is complying with the same approach as widely used in [23], [46], [47], [48].

The representative case of *level-1* social communications is described in Fig. 4(c), and the corresponding symbols in the model are listed in Fig. 4(d). The destination user v_k is chosen among the four *level-1* contacts (user v_j). In *level-L* ($L = 2, 3, \dots, L_{max}$) situations, the pattern is almost the same except that the destination user is re-selected among the *level-L* contacts.

Similar to the approaches widely used in [23], [46], [47],

[48], a simple multi-hop routing scheme in the physical space domain is adopted here. When the source user is about to send a data packet, it chooses one user closest to its destination user from its neighboring squares to relay the packet. This kind of physical relaying steps keep going until the data packet eventually reaches the destination user after multiple hops. The red dotted line with arrows denotes one possible routing path in Fig. 4(c). The data packet can be successfully transported for any pair of transmission under the condition that there is at least one user in each square. Surely this condition can be satisfied with a probability approaching 1 according to the classical work in [46]. In Fig. 4(c), since every hop transmits the packet from one small square to one of its neighboring squares, all the squares marked in red solid have the same hops x from the source user as the destination user v_k , and the total number of hops is $4x$. The radius R_1 and R_2 of the two dotted-line circles are used as the indicative distances between the source and destination user instead of their real distance.

Corresponding to the D2D social communication scenario, the widely employed protocol model in [23], [46], [60] is adopted as the measurement of a successful physical transmission. Firstly, as mentioned above, two users can exchange contents directly only when they are geographically close enough in the D2D communication, so an upper bound of the distance has to be set between two users who can physically communicate directly. Secondly, interference is one of the main issues to be paid attention to in the D2D communication. In order to rule out the influence of interference, the distance between the transmitter and the receiver has to meet some lower bound. According to the above protocol model, a physical transmission is successful if and only if the Euclidean distance between two users meets the conditions: $|X_i - X_j| \leq r(n)$ and $|X_k - X_i| \geq (1 + \Delta)|X_i - X_j|$, where X_i and X_j refer to the transmitter and the receiver respectively, X_k denotes any other transmitter sharing the same channel with X_i and Δ is the guard zone factor. It has been proven that the transmission range $r(n)$ must reach $\Theta\left(\sqrt{\frac{\log n}{n}}\right)$ to guarantee the connectivity of the network [61]. In Fig. 4(c), the solid-line circle with the radius of $r(n)$ displays the transmission range.

For keeping consistence with the above protocol model in analyzing the capacity, similarly to [20], [46], a TDMA (Time Division Multiple Access) scheme is designated as the MAI (multiple access interference) avoidance method. As shown in Fig. 4(c), the networking area is divided into a number of smaller squares with side length $C_1 r(n)$, where C_1 is a constant. Equivalent to the condition $|X_k - X_i| \geq (1 + \Delta)|X_i - X_j|$ in the classical protocol model, the interference units refer to those squares containing at least two nodes closer than $(2 + \Delta)r(n)$ respectively [20], and these squares which can simultaneously transmit data packets should not be the interference units with each other. Therefore, users in the squares signed with blue stars in Fig. 4(c), which are at least T squares away from each other, are permitted to transmit data packets at the same time, where $T \geq (2 + \Delta)/C_1$.

Since the selection rule of the destination user affects the

capacity of the fractal D2D social network as well, two destination user selection rules are adopted in this paper, namely, the uniform distribution and the power-law distribution. Actually, these two patterns have been widely used in a large amount of research on the social network as the distributions of destination users, such as [23], [47], [48]. In the first case, the destination user is selected according to the uniform distribution. That is to say, a user communicates with one of his/her contacts in a random manner, and all the potential contacts have the equal opportunity to communicate with the user. This mode should be considered analytically reasonable because it is the most natural and the fairest way without additional knowledge about the social preference of the users. In the second case, the destination user is selected according to the power-law distribution $d^{-\beta}$ [62], where d refers to the distance between the source and destination user, and β is the frequency parameter. This selection rule is considered to be practically reasonable as Latane *et al.* [62] discovered that a user prefers to communicate with physically closer user among his/her social contacts, and the probability is proportional to the power-law of the distance. In other words, the social contacts closer to the source user have more opportunities to communicate with him/her. Therefore, these two destination selection rules adopted in this paper make sense in a social network setting.

For simplicity of representation, some essential definitions are given and the relationship between them is highlighted as following.

Definition 1. The elementary symmetric polynomial [63] $\sigma_{p,N}(Q')$, $1 \leq p \leq N$ of variables $Q' = (q_1, q_2, \dots, q_N)$ is noted as

$$\begin{aligned} \sigma_{p,N}(Q') &= \sigma_{p,N}(q_1, q_2, \dots, q_N) \\ &= \sum_{1 \leq i_1 \leq i_2 \leq \dots \leq i_p \leq N} q_{i_1} q_{i_2} \dots q_{i_p}. \end{aligned}$$

Definition 2. The elementary symmetric polynomial [63] $\bar{\sigma}_{p,N-1}^k(Q')$, $1 \leq p \leq N-1$ of variables $Q' = (q_1, q_2, \dots, q_N)$ except q_k is noted as

$$\bar{\sigma}_{p,N-1}^k(Q') = \sigma_{p,N-1}(q_1, q_2, \dots, q_{k-1}, q_{k+1}, \dots, q_N).$$

From [23], [63], we can have the following lemma.

Lemma 1. Let the set $Q' = \{q_1, q_2, \dots, q_N\}$ contains $N \geq 2$ non-negative real numbers. If q is finite, then we have [63]:

$$\frac{\sigma_{1,N}(Q') \cdot \sigma_{q,N}(Q')}{(q+1) \cdot \sigma_{q+1,N}(Q')} = \Theta\left(\frac{N}{N-q}\right).$$

To be clear, it turns out that the symbol Θ is not about the numerical value, it is about the speed of growth. In other words, two variables on the two sides of an equation have the same speed of growth.

III. THE UPPER BOUND OF THE CAPACITY WITH DIRECT SOCIAL COMMUNICATIONS

In this section, the aforementioned properties of fractal D2D social networks are followed and the specific derivation procedure of the maximum capacity with direct social communications is clarified. That is to say, only the *level-1* social communication is considered in this section, and all

the contacts, degrees, degree distribution or joint probability distribution in this section are default *level-1*. In addition, the impact of a particular destination selection rule on the maximum achievable throughput is studied by taking account of two different cases, including uniformly and power-law distributed destinations.

For the convenience for understanding, a list of all the symbols and their explanations is shown in Table I.

TABLE I: The list of the symbols and their meanings in Section III.

Symbols	Meanings
n	The total number of users.
k	The degree of a user.
q	The degree of the source user.
q_0	A relative large degree to divide the range of degrees into two parts.
N	The number of potential contacts whose degree is less than q .
γ	The degree distribution exponent of a fractal network.
ϵ	The correlation exponent of a fractal network.
$M_{\gamma,\epsilon}$	The normalization constant in the joint probability distribution $P(k_1, k_2)$.
\mathbf{C}	The set of all <i>level-1</i> contacts.
v_i	The source user.
v_t	The destination user.
v_k	A particular contact who is selected as the destination user.
q_k	The degree of v_k .
λ	The data rate for every user.
λ_{max}	The maximum achievable capacity.
X	The number of hops from the source user to the destination user.
$E[X]$	The average number of hops.
E_1	The average number of hops when $q \leq q_0$ under the case of uniformly distributed destinations.
E_2	The average number of hops when $q > q_0$ under the case of uniformly distributed destinations.
s_l	The red squares in Fig. 4(c), where $l = 1, 2, \dots, 4x$.
d	The distance between the source user and the destination user.
d_j	The distance between the source user and his j -th contact.
β	The frequency parameter.
E_3	The average number of hops when $q \leq q_0$ under the case of power-law distributed destinations.
E_4	The average number of hops when $q > q_0$ under the case of power-law distributed destinations.

A. The Case of Uniformly Distributed Destinations

In the first case, the uniform distribution of the destination users is considered. In other words, the source user selects one of his/her *level-1* contacts as the destination user randomly. In this situation, the result of the maximum capacity is given in Theorem 1 and proven afterwards. It is noteworthy that the proof may seem similar as [23], but actually totally different in details because the capacity of fractal networks is focused on here.

Theorem 1. For a fractal D2D social network with n users satisfying the conditions below: 1) the *level-1* social contacts are selected according to the joint probability distribution $P(k_1, k_2) = \frac{k_1^{-(\gamma-1)} k_2^{-\epsilon}}{M_{\gamma, \epsilon}}$, ($k_1 > k_2$), where $M_{\gamma, \epsilon}$ is the normalization constant; 2) the *level-1* degree of each user follows the power-law degree distribution $P(k) = \frac{k^{-\gamma}}{\sum_{k=1}^n k^{-\gamma}}$; 3) the destination user v_t is chosen by the source user v_i according to the uniform distribution $P(v_t = v_k | v_k \in \mathbf{C}) = \frac{1}{q}$, where q is the *level-1* degree of the source user, \mathbf{C} is the set of all *level-1* contacts, and v_k is a particular contact who is selected as the destination user. Then the maximum capacity λ_{max} of the fractal D2D social network with direct social communications is

$$\lambda_{max} = \Theta\left(\frac{1}{\sqrt{n \cdot \log n}}\right), \quad (4)$$

where the symbol Θ refers to the order of magnitude.

Before giving the proof, some key lemmas are listed as follows. First, from [23], we can have the following lemma.

Lemma 2. Assume that λ is the data rate for every user, λ_{max} is the maximum capacity of the fractal D2D social network. X is the number of hops from the the source user to the destination user. $E[X]$ denotes the expectation of X for any social transmission pair. Then we have

$$\lambda \leq \lambda_{max} = \Theta\left(\frac{1}{\log n \cdot E[X]}\right). \quad (5)$$

Lemma 3. Let the degree of the source user be q , where $q = 1, 2, \dots, n$. v_k is a particular contact who is selected as the destination user, and q_k is the degree of v_k . The variables $q_{i_1}, q_{i_2}, \dots, q_{i_N}$ in $Q = (q_{i_1}^{-\epsilon}, q_{i_2}^{-\epsilon}, \dots, q_{i_N}^{-\epsilon})$ denote the degrees of N potential *level-1* social contacts whose degree are smaller than q . x is the number of hops from the source to the destination user, and s_l ($l = 1, 2, \dots, 4x$) stands for the red square in Fig. 4(c). Then the average number of hops is

$$E[X] = \sum_{q=1}^n \frac{q^{-\gamma}}{\sum_{b=1}^n b^{-\gamma}} \cdot \sum_{x=1}^{\frac{1}{r(n)}} x \sum_{l=1}^{4x} \sum_{v_k \in s_l} \frac{q_k^{-\epsilon} \cdot \sigma_{q-1, N-1}^k(Q)}{q \cdot \sigma_{q, N}(Q)}. \quad (6)$$

The proof is left in Appendix A.

Next, $E[X]$ is divided into two separate cases E_1 and E_2 with a boundary q_0 , which is a constant and indicates a relatively large degree. E_1 is the average number of hops when $q \leq q_0$, where the degree q of the source user is a finite integer, meanwhile E_2 is the average number of hops when $q > q_0$, where q is considered to be infinite.

Lemma 4. When the degree of the source user is not greater than q_0 , i.e., $q \leq q_0$, the average number of hops E_1

is

$$E_1 = \Theta\left(r(n)^{-1}\right). \quad (7)$$

Proof: According to the meaning of E_1 , it can be given as

$$E_1 = \sum_{q=1}^{q_0} \frac{q^{-\gamma}}{\sum_{b=1}^n b^{-\gamma}} \cdot \sum_{x=1}^{\frac{1}{r(n)}} x \sum_{l=1}^{4x} \sum_{v_k \in s_l} \frac{q_k^{-\epsilon} \cdot \sigma_{q-1, N-1}^k(Q)}{q \cdot \sigma_{q, N}(Q)}. \quad (8)$$

All situations of selecting $q-1$ users from \mathbf{C} can be parted into two categories according to the condition whether v_k is chosen or not. If it is chosen, other $q-2$ users have to be chosen from \mathbf{C} besides v_k . Otherwise $q-1$ users are chosen in \mathbf{C} except v_k . That is to say,

$$\begin{aligned} \sigma_{q-1, N-1}^k(Q) &= \sigma_{q-1, N}(Q) - q_k^{-\epsilon} \cdot \sigma_{q-2, N-1}^k(Q) \\ &= \sigma_{q-1, N}(Q) - q_k^{-\epsilon} \left(\sigma_{q-2, N}(Q) - q_k^{-\epsilon} \cdot \sigma_{q-3, N-1}^k(Q) \right). \end{aligned}$$

Since every term above is positive, then we have

$$\sigma_{q-1, N}(Q) - q_k^{-\epsilon} \cdot \sigma_{q-2, N}(Q) < \sigma_{q-1, N-1}^k(Q) < \sigma_{q-1, N}(Q). \quad (9)$$

According to Eq. (9), it turns out the upper bound and the lower bound have the same order:

$$E_1 = O\left(r(n)^{-1}\right), \quad E_1 = \Omega\left(r(n)^{-1}\right). \quad (10)$$

The proof of Eq. (10) in details is in Appendix B and now Lemma 4 is proven. ■

Lemma 5. When the degree of the source user is greater than q_0 , i.e., $q > q_0$, the average number of hops E_2 is

$$E_2 = \Theta\left(r(n)^{-1}\right). \quad (11)$$

The proof is left in Appendix C.

Now Theorem 1 can be proven.

Proof: In order to get the result in Theorem 1, the proof sketch below inspired by [23] is followed. Firstly, the relationship between the capacity and the average number of hops $E[X]$ is presented in Lemma 2, so the problem can be solved by finding out $E[X]$. Secondly, the expression of $E[X]$ is given in Lemma 3. Thirdly, $E[X]$ is separated into two cases E_1 and E_2 according to the boundary q_0 , and E_1 and E_2 are obtained respectively. Therefore, the capacity derivation can be achieved by backtracking. Based on the results in Lemma 4 and Lemma 5,

$$E[X] = E_1 + E_2 = \Theta\left(r(n)^{-1}\right). \quad (12)$$

Together with Lemma 2, the results in Theorem 1 is obtained. ■

B. The Case of Power-law Distributed Destinations

In the second case, it is assumed that the probability that the source user communicates with one of his/her *level-1* contacts is proportional to $d^{-\beta}$, where d refers to the distance between two users and β indicates that the closer contacts have more opportunities to communicate with the source user. The fractal D2D social network achieves another maximum throughput in this situation, which is clarified in Theorem 2.

Theorem 2. For a fractal D2D social network with n users satisfying the conditions below: 1) the social contacts are selected according to the joint probability distribution $P(k_1, k_2) = \frac{k_1^{-(\gamma-1)} k_2^{-\epsilon}}{M_{\gamma, \epsilon}}$, ($k_1 > k_2$), where $M_{\gamma, \epsilon}$ is the normalization constant; 2) the degree of each user follows the power-law degree distribution $P(k) = \frac{k^{-\gamma}}{\sum_{k=1}^n k^{-\gamma}}$; 3) the destination user v_t is chosen according to the power-law distribution $P(v_t = v_k | v_k \in \mathbf{C}) = \frac{d^{-\beta}}{\sum_{j=1}^q d_j^{-\beta}}$, where \mathbf{C} is the set of all contacts, v_k is a particular contact who is selected as the destination user, d is the distance from the source user to the destination user, d_j is the distance between the source user and his j -th contact, and β is the frequency parameter. Then the maximum capacity λ_{max} of the fractal D2D social network is

$$\lambda_{max} = \begin{cases} \Theta\left(\frac{1}{\sqrt{n \cdot \log n}}\right), & 0 \leq \beta \leq 2; \\ \Theta\left(\frac{1}{\sqrt{n^{3-\beta} \cdot \log n^{\beta-1}}}\right), & 2 < \beta < 3; \\ \Theta\left(\frac{1}{\log n}\right), & \beta \geq 3. \end{cases} \quad (13)$$

The proof of Theorem 2 is pretty similar to Theorem 1, so only the relevant key lemmas in the derivation procedure are given.

Lemma 6. Let the degree of the source user be q , where $q = 1, 2, \dots, n$. v_k is a particular contact who is selected as the destination user. q_k is the degree of v_k and d_k is the distance from the source user to v_k . The variables $q_{i_1}, q_{i_2}, \dots, q_{i_N}$ in $Q = (q_{i_1}^{-\epsilon}, q_{i_2}^{-\epsilon}, \dots, q_{i_N}^{-\epsilon})$ denote the degrees of N potential *level-1* social contacts whose degree are smaller than q . Let $D = (d_1^{-\beta}, d_2^{-\beta}, \dots, d_q^{-\beta})$, where d_j ($1 \leq j \leq q$) in D denotes the distance between the j -th social contact and the source user. Then the average number of hops is

$$E[X] = \sum_{q=1}^n \frac{q^{-\gamma}}{\sum_{b=1}^n b^{-\gamma}} \cdot \sum_{x=1}^{\frac{1}{r(n)}} x \sum_{l=1}^{4x} \sum_{v_k \in s_l} \frac{q_k^{-\epsilon} \cdot \sigma_{q-1, N-1}^k(Q)}{\sigma_{q, N}(Q)} \cdot \frac{d_k^{-\beta}}{\sigma_{1, q}(D)}. \quad (14)$$

Lemma 7. When the degree of the source user is not greater than q_0 , i.e., $q \leq q_0$, the average number of hops E_3 is

$$E_3 = \begin{cases} \Theta\left(r(n)^{-1}\right), & 0 \leq \beta \leq 2; \\ \Theta\left(r(n)^{\beta-3}\right), & 2 < \beta < 3; \\ \Theta(1), & \beta \geq 3. \end{cases} \quad (15)$$

Lemma 8. When the degree of the source user is greater than q_0 , i.e., $q > q_0$, the average number of hops E_4 is

$$E_4 = \begin{cases} \Theta\left(r(n)^{-1}\right), & 0 \leq \beta \leq 2; \\ \Theta\left(r(n)^{\beta-3}\right), & 2 < \beta < 3; \\ \Theta(1), & \beta \geq 3. \end{cases} \quad (16)$$

Combine Lemma 2 with Lemma 7 and Lemma 8, the result

in Theorem 2 is obtained.

IV. THE UPPER BOUND OF THE CAPACITY WITH HIERARCHICAL SOCIAL COMMUNICATIONS

In the last section, the case with direct social communications is taken into account. However, as we mention earlier, the social communications can actually be hierarchical with multiple social levels through the inter-connected users. In other words, the source user can communicate with one of his/her *level-L* ($L = 1, 2, \dots, L_{max}$) contacts through $L - 1$ inter-users. In this section, the relationship between the extendibility of a fractal social network and the correlation exponent ϵ is first given in Theorem 3. Then the results achieved in the last section are extended to the case with hierarchical social communications in Theorem 4.

Theorem 3. For a fractal D2D social network with n users satisfying the conditions below: 1) the *level-1* contacts are selected according to the joint probability distribution $P(k_1, k_2) = \frac{k_1^{-(\gamma-1)} k_2^{-\epsilon}}{M_{\gamma, \epsilon}}$, ($k_1 > k_2$); 2) the *level-1* degree of each user follows the power-law degree distribution $P(k) = \frac{k^{-\gamma}}{\sum_{k=1}^n k^{-\gamma}}$. According to the definition given above, the relationship between the extendibility of the fractal network and the correlation exponent ϵ is:

1) If $2 < \epsilon < 3$, the fractal network can expand its branches continuously, and the average *level-L* ($L = 1, 2, \dots, L_{max}$) degree increases monotonously via expanding.

2) $\epsilon = 3$ is the boundary to distinguish whether the fractal network is extensible or not. In this case, the mean of *level-L* degree keeps invariant throughout.

3) If $\epsilon > 3$, the fractal network will stop branching rapidly after expanding finite levels. In other words, the expectation of *level-L* degree decreases monotonously.

Proof: Only some key elements are provided here for better readability, and the proof of Theorem 3 in details can be found in Appendix D.

Let $K^{(L)}$ denote the *level-L* ($L = 1, 2, \dots, L_{max}$) degree of one user, and $\bar{K}^{(L)}$ is the expectation of $K^{(L)}$.

As depicted in Fig. 2(b), assume the *level-1* degree of Alice is known to be $K^{(1)}$, and the crucial variable here is the average *level-L* degree $\bar{K}^{(L)}$ of Alice.

It turns out that the average *level-2* degree $\bar{K}^{(2)}$ is:

$$\bar{K}^{(2)} = \frac{1}{\epsilon - 2} \cdot \frac{\gamma - 1}{\gamma - 2}.$$

When $L \geq 3$, the average *level-L* degree can be derived in a similar way. Consequently, the average *level-L* degree can be written as:

$$\bar{K}^{(L)} = \frac{1}{\epsilon - 2} \cdot \bar{K}^{(L-1)}.$$

Therefore, the final expression of $\bar{K}^{(L)}$ is obtained:

$$\bar{K}^{(L)} = \left(\frac{1}{\epsilon - 2}\right)^{L-1} \cdot \frac{\gamma - 1}{\gamma - 2}, \quad L = 1, 2, \dots, L_{max}. \quad (17)$$

Now from Eq. (17), it can be seen that the conclusion in Theorem 3 holds. ■

Additionally, for the convenience of understanding, the conclusions on the extendibility features in Theorem 3 are

depicted in Fig. 5. As we know, self-similarity is one of the most important features of fractality. In other words, a fractal network has identical characteristics in any scale. Intuitively, the extendibility of fractal networks can be understood by imagining the growth of a fractal network, which starts from a central node and keep stretching out the branches in the same pattern. The correlation exponent ϵ describes the extent of fractality and decides the pattern of the stretching branches. According to the mathematical derivation in this paper, $\frac{1}{\epsilon-2}$ indicates the number of connections in a branch in the statistical sense. Hence, this expression has no practical significance when $\epsilon \leq 2$, and the number of connections in a branch is less than one when $\epsilon > 3$, thus the network is unable to keep the growing tendency of stretching out. Therefore, the correlation exponent ϵ has to fall in the range of $(2, 3]$ from the mathematical and practical point of view.

As illustrated in Fig. 5, the fractal network keeps branching when $2 < \epsilon < 3$, thus the expectation of *level-L* degree $\overline{K}^{(L)}$ keeps rising. Specifically, the *level-1* degree of v_i is 4 while the *level-2* degree increases to 8 as the dotted connections in Fig. 5(a) show. The $\overline{K}^{(L)}$ remains invariant if $\epsilon = 3$, it can be seen from the consistent *level-L* degree of v_i in Fig. 5(b), which is always 4. While the expectation of degree reduces to 0 quickly when $\epsilon > 3$ because the factor $\frac{1}{\epsilon-2}$ is smaller than 1 in this case. As a result, the degree of v_i falls from 4 to 2 after the expanding of one level in Fig. 5(c).

Actually, it has been discovered in documents that the correlation exponent is usually in the range $2 < \epsilon < 3$ in real complex networks [14], which validates the correctness of the mathematical derivation in this work.

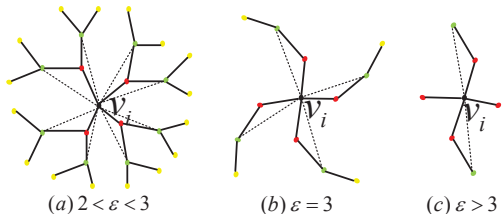


Fig. 5: The extendibility of a fractal network under different values of correlation exponent ϵ .

Theorem 4. For a fractal D2D social network with n users satisfying the conditions below: 1) the *level-1* contacts are selected according to the joint probability distribution $P(k_1, k_2) = \frac{k_1^{-(\gamma-1)} k_2^{-\epsilon}}{M_{\gamma, \epsilon}}$, ($k_1 > k_2$); 2) the *level-1* degree of each user follows the power-law degree distribution $P(k) = \frac{k^{-\gamma}}{\sum_{k=1}^{\lambda_{max}} k^{-\gamma}}$. Then the maximum capacity $\lambda_{max}^{(H)}$ of the fractal D2D social network with hierarchical communications is

$$\lambda_{max}^{(H)} = \begin{cases} \Theta\left(\lambda_{max} \cdot \frac{1}{\log n}\right), & 2 < \epsilon < 3; \\ \Theta(\lambda_{max} \cdot n^{-1}), & \epsilon = 3. \end{cases} \quad (18)$$

where λ_{max} refers to the maximum capacity of fractal D2D social networks with direct communications as defined in Theorem 1 or Theorem 2 in Section III. Note that Theorem 4 holds for both uniform and power-law destination selection cases.

Proof: Taking the social communications of all levels in a fractal D2D social network into consideration, the average number of hops $E^{(H)}[X]$ to the destination user of arbitrary hierarchical level is

$$E^{(H)}[X] = E^{(1)}[X] \cdot R^{(1)} + \dots + E^{(L_{max})}[X] \cdot R^{(L_{max})}, \quad (19)$$

where $E^{(L)}[X]$ ($L = 1, 2, \dots, L_{max}$) refers to the average number of hops in the case of *level-L* social communications. Specifically, $E^{(1)}[X]$ is the same as the aforementioned $E[X]$. The approximate relationship between $E^{(L)}[X]$ and $E^{(1)}[X]$ generally holds: $E^{(L)}[X] \approx L \cdot E^{(1)}[X]$. In addition, $R^{(L)}$ ($L = 1, 2, \dots, L_{max}$) stands for the ratio between the numbers of contact pairs of *level-L* and that of all levels.

Define $m^{(L)}$ ($L = 1, 2, \dots, L_{max}$) to be the number of edges in the *level-L* graph, which is formed by connecting all *level-L* contact pairs virtually as illustrated in Fig. 3. From now on $R^{(L)}$ is derived.

The average degree $\overline{K}^{(L)}$ and the number of edges $m^{(L)}$ meet the equation below [64]:

$$m^{(L)} = \overline{K}^{(L)} \cdot n/2.$$

The total number of contact pairs of all levels is $\binom{n}{2}$, then the proportion of *level-L* contact pairs is:

$$R^{(L)} = m^{(L)} / \binom{n}{2} = \frac{\overline{K}^{(L)}}{n-1}.$$

Due to the possible existence of loops in fractal D2D social networks, some contact pairs may be counted repeatedly. For instance, hub_A and hub_B in Fig. 1 can be seen as a *level-1* contact pair or a *level-4* contact pair. As a result, we define a maximum level L_{max} to imply that the contact pairs with levels larger than L_{max} have been counted before.

Now the maximum capacity under the condition of $2 < \epsilon < 3$ and $\epsilon = 3$ is discussed, respectively. Define $\alpha = \frac{1}{\epsilon-2}$ for the simplicity of the expressions.

Case 1: $2 < \epsilon < 3$, i.e., $\alpha > 1$

As we know, the summation of $R^{(L)}$ should equal to one:

$$\begin{aligned} \sum_{l=1}^{L_{max}} R^{(l)} &= \frac{\gamma-1}{(\gamma-2)(n-1)} (1 + \alpha + \dots + \alpha^{L_{max}-1}) \\ &= \frac{(\gamma-1)}{(\gamma-2)(\alpha-1)(n-1)} \cdot (\alpha^{L_{max}} - 1) \\ &= 1. \end{aligned} \quad (20)$$

So the maximum level can be calculated as:

$$L_{max} = \frac{\log\left[\frac{(\gamma-2)(\alpha-1)(n-1)}{(\gamma-1)} + 1\right]}{\log(\alpha)} = \Theta(\log n). \quad (21)$$

According to Eq. (19), the average number of hops $E^{(H)}$

in this case is:

$$\begin{aligned}
E^{(H)}[X] &= \sum_{l=1}^{L_{\max}} E^{(l)}[X] \cdot R^{(l)} \\
&= \sum_{l=1}^{L_{\max}} E^{(1)}[X] \cdot l \cdot \frac{\gamma-1}{(\gamma-2)(n-1)} \cdot \alpha^{l-1} \\
&= E^{(1)}[X] \cdot \frac{\gamma-1}{(\gamma-2)(n-1)} \sum_{l=1}^{L_{\max}} l \cdot \alpha^{l-1} \\
&= E^{(1)}[X] \cdot \frac{\gamma-1}{(\gamma-2)(n-1)} \cdot S,
\end{aligned}$$

where $S = \sum_{l=1}^{L_{\max}} l \cdot \alpha^{l-1}$, and it can be given analytically according to Eq. (20):

$$\begin{aligned}
S &= \frac{1}{\alpha-1} \cdot L_{\max} \cdot \left(\frac{(\gamma-2)(\alpha-1)(n-1)}{\gamma-1} + 1 \right) \\
&\quad - \frac{1}{\alpha-1} \cdot \frac{(\gamma-2)(n-1)}{\gamma-1}.
\end{aligned}$$

According to the order of L_{\max} in Eq. (21),

$$\frac{\gamma-1}{(\gamma-2)(n-1)} \cdot S = \Theta(\log n).$$

Then we can have:

$$E^{(H)}[X] = \Theta \left(E^{(1)}[X] \cdot \log n \right). \quad (22)$$

Combining Eq. (22) with Lemma 2, the maximum capacity with hierarchical social communications in the case $2 < \epsilon < 3$ is obtained:

$$\lambda_{\max}^{(H)} = \Theta \left(\lambda_{\max} \cdot \frac{1}{\log n} \right). \quad (23)$$

Case 2: $\epsilon = 3$, i.e., $\alpha = \frac{1}{\epsilon-2} = 1$.

In this case,

$$R^{(L)} = \frac{\gamma-1}{(\gamma-2)(n-1)} = R^{(1)}.$$

So the maximum level is calculated as:

$$L_{\max} = \frac{1}{R^{(1)}} = \frac{(\gamma-2)(n-1)}{\gamma-1} = \Theta(n).$$

According to Eq. (19), the average number of hops $E^{(H)}$ is:

$$\begin{aligned}
E^{(H)}[X] &= \sum_{l=1}^{L_{\max}} E^{(l)}[X] \cdot R^{(l)} \\
&= E^{(1)}[X] \cdot R^{(1)} \cdot \sum_{l=1}^{L_{\max}} l \\
&= E^{(1)}[X] \cdot \frac{(\gamma-2)n+1}{2(\gamma-1)}.
\end{aligned}$$

So the average number of hops is obtained:

$$E^{(H)}[X] = \Theta \left(E^{(1)}[X] \cdot n \right). \quad (24)$$

In other words, the maximum capacity in this case is:

$$\lambda_{\max}^{(H)} = \Theta(\lambda_{\max} \cdot n^{-1}). \quad (25)$$

To sum up Eq. (23) and Eq. (25), the maximum capacity $\lambda_{\max}^{(H)}$ of fractal D2D social networks with hierarchical communications in Theorem 4 is achieved. ■

V. NUMERICAL SIMULATIONS AND DISCUSSIONS

In this section, the theoretical results in Theorem 1, Theorem 2 and Theorem 4 are illustrated in an intuitive manner, and the theoretical capacity bound is compared with the experimental results.

The network capacity in direct social communications scenario is illustrated by the dotted lines in Fig. 6. When β varies within $[0, 2]$, the average number of hops does not decrease distinctly compared with the uniform destination selection case. When β changes between $(2, 3)$, the source user prefers to communicate with closer direct social contacts, which leads to the exponentially growth of the maximum throughput. After β rises to 3, only $\Theta(1)$ average hops are taken for each social transmission, which raises the maximum capacity with direct communications up to $\Theta\left(\frac{1}{\log n}\right)$ finally. The results are also consistent with our findings in Theorem 2.

In order to test the tightness of the theoretical results in our work, the simulations are conducted as follows. Firstly, the social connections are determined according to the two aforementioned power-law distributions, namely, $P(k)$ and $P(k_1, k_2)$, thus a fractal social network is formed with a connection matrix \mathbf{A} containing the connection relationships among all users. Secondly, all users are scattered in a square with the unit area and their positions are assigned according to the uniform distribution. Next, the decision is made on which users are allowed to transmit data simultaneously based on the system model in Section II-C. Then for each user in the last step, a destination is chosen in his/her contact user matrix on the basis of uniform or power-law distribution under different destination selection rules, and the number of hops is calculated through the positions of the source-and-destination pair and the side length of each small square. Finally, the average of hops is obtained, thus the capacity can be achieved according to Theorem 2. For the enhancement of understanding, all parameters in the simulation and their settings are listed in Table II below.

As shown in Fig. 6, the theoretical capacity bound is compared with the experimental results in the case of direct social communications. It is observed that no matter in the uniform or power-law case with different values of β , the simulation curve is very similar with the theoretical one with respect to growing tendency, which matters most in our comparison because the analytical results in this paper focus on the order of magnitude instead of the magnitude itself. Therefore, the tightness of the mathematical derivation in this paper is validated.

In addition to the impact of the number of users, other performance metrics are also investigated. As seen from Table II, the transmission range and the average distance between two adjacent users change as the variation of n , and the influence brought by these two parameters in both the uniform and power-law cases are depicted in Fig. 7 and Fig. 8, respectively. Basically, the maximum capacity goes downwards as the average distance between two adjacent users or the

TABLE II: The list of the parameters in the simulation and their settings.

Parameter	Setting
The area of the square system $area$	1
The total number of users n	[100,1000]
The transmission range $r(n)$	$\sqrt{\frac{\log n}{n}}$
The average distance between two adjacent users $Distance$	$\sqrt{\frac{1}{n}}$
The side length of the small squares $side_length$	$\sqrt{\frac{\log n}{n}}$
The number of small squares between cells that can transmit simultaneously T	3
The guard factor Δ	1
The degree distribution exponent γ	2.5
The correlation exponent ϵ	2.5

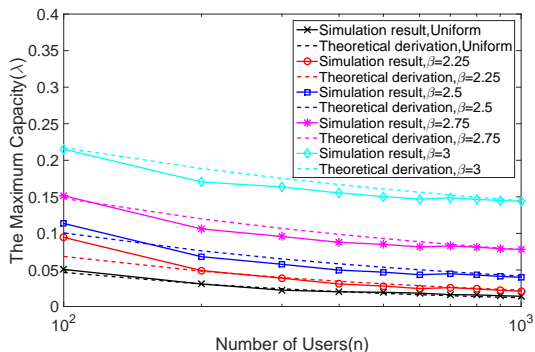


Fig. 6: Comparison between the theoretical capacity bound and the experimental results in the case of direct social communications with respect to the number of users.

transmission range decreases. It is consistent with the actual D2D networking situation because the transmission range has to shrink to mitigate the severe interference as the users get crowded. As a result, the side length of each small squares in the system model shrinks too and it takes more hops to finish one transmission. Finally, the capacity is cut down.

Next, the effect of the correlation exponent ϵ on the achievable capacity is discussed. According to Theorem 4, corresponding to different values of the correlation exponent ϵ , the hierarchical social communications reduce the achievable capacity, which implies the improved security level at the cost of the capacity attenuation of fractal D2D social communications. The reduction proportion is $\frac{1}{\log n}$ if $2 < \epsilon < 3$ and $\frac{1}{n}$ if $\epsilon = 3$, compared to that with direct social communications. The effects of reduction under two different destination selection means (i.e., uniform and power-law) are provided in Fig. 9 and Fig. 10, respectively. Specifically, it shows that the order of the maximum capacity is reduced by $\frac{1}{\log(n)}$ when the correlation exponent ϵ is within the range (2, 3), while the reduction factor is $\frac{1}{n}$ when the correlation exponent $\epsilon = 3$.

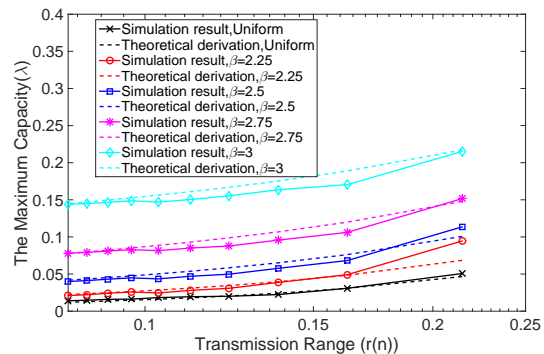


Fig. 7: Comparison between the theoretical capacity bound and the experimental results in the case of direct social communications with respect to the transmission range.

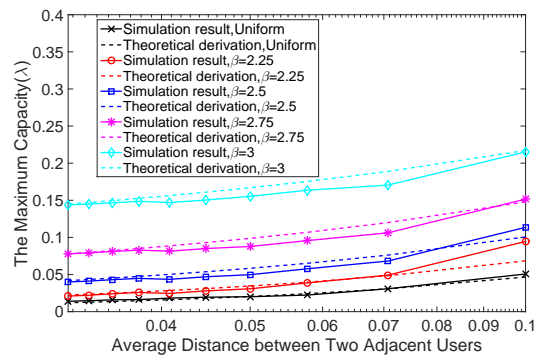


Fig. 8: Comparison between the theoretical capacity bound and the experimental results in the case of direct social communications with respect to the average distance between two adjacent users.

The reduction effect can be seen as a trade-off between the security level and achievable capacity of fractal D2D social networks, and the attenuation on the maximum capacity can be intuitively explained by the topological extension feature of fractal social networks. As is mentioned in Section II, the logarithm of the number of boxes $N_B(l_B)$ is linearly dependent on the length scale l_B , which indicates the possible existence of box extension with a very large size. In other words, the fractal topology stretches out the path between some social transmission pairs, which leads to the increase of the average number of hops in the scenario with hierarchical social communications, and results in the reduction on the maximum achievable capacity naturally.

VI. CONCLUSION AND FUTURE WORKS

In this paper, the maximum capacity of fractal D2D social networks with both direct and hierarchical communications is studied.

Under the condition of direct social communications, it has been proven that if the source user communicates with one of his/her direct contacts randomly, the maximum capacity in Theorem 1 corresponds to the classical result $\Theta\left(\frac{1}{\sqrt{n \log n}}\right)$ achieved by Kumar [20]. On the other hand, if the two users

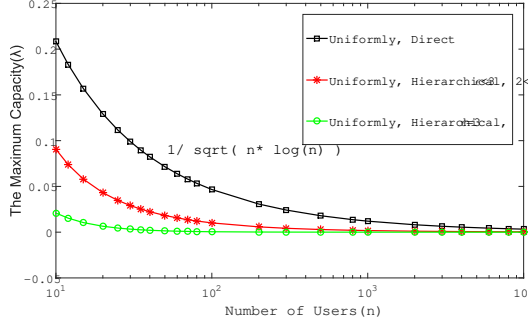


Fig. 9: The comparison between the maximum capacity of fractal D2D social networks with hierarchical and direct communications under the case of uniformly distributed destinations.

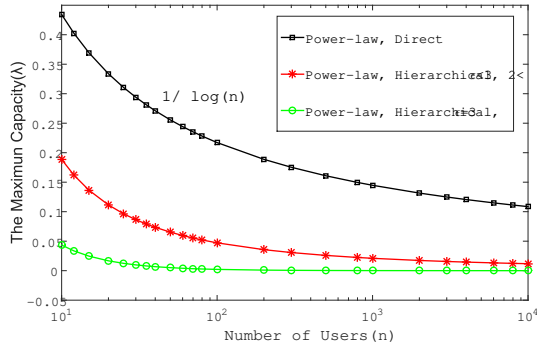


Fig. 10: The comparison between the maximum capacity of fractal D2D social networks with hierarchical and direct communications under the case of power-law distributed destinations.

with distance d communicate with each other according to the probability in proportion to $d^{-\beta}$, the maximum capacity is

$$\lambda_{\max} = \begin{cases} \Theta\left(\frac{1}{\sqrt{n \cdot \log n}}\right), & 0 \leq \beta \leq 2; \\ \Theta\left(\frac{1}{\sqrt{n^{3-\beta} \cdot \log n^{\beta-1}}}\right), & 2 < \beta < 3; \\ \Theta\left(\frac{1}{\log n}\right), & \beta \geq 3. \end{cases}$$

While taking social communications of all levels into account, for both uniform and power-law destination selection cases, it is discovered that the hierarchical social communications further decrease the respective maximum capacity in a proportion related to the number of users n , and the corresponding reduction factor varies by different values of the correlation exponent ϵ of the fractal D2D social networks:

$$\lambda_{\max}^{(H)} = \begin{cases} \Theta\left(\lambda_{\max} \cdot \frac{1}{\log n}\right), & 2 < \epsilon < 3; \\ \Theta(\lambda_{\max} \cdot n^{-1}), & \epsilon = 3. \end{cases}$$

Surely, there are still some issues remain to be solved in the future studies. For instance, why the condition $\epsilon = 3$ is

the boundary to determine whether or not the fractal network is extensible. Moreover, why is there a leap in the reduction coefficient of hierarchical social communications when $\epsilon = 3$. We leave all these open issues in the future works.

APPENDIX

A. Proof of Lemma 3

Let $P(k = q)$ denote the probability that the degree of the source user is q , while $E[X|\text{source } v_i, k = q]$ is the average number of hops under the condition that the source user v_i has q contacts, then $E[X]$ can be written as

$$E[X] = \sum_{q=1}^n P(k = q) \cdot E[X|\text{source } v_i, k = q]. \quad (26)$$

Let $P(X = x)$ denote the probability of x hops ranging from 1 to $1/r(n)$. The event $X = x$ is true if and only if v_k locates in the red squares s_l ($l = 1, 2, \dots, 4x$) in Fig. 2(c) and is selected as the destination user v_t . Therefore, $E[X|\text{source } v_i, k = q]$ can be expanded as

$$\begin{aligned} E[X|\text{source } v_i, k = q] &= \sum_{x=1}^{\frac{1}{r(n)}} x \cdot P(X = x) \\ &= \sum_{x=1}^{\frac{1}{r(n)}} x \cdot \sum_{l=1}^{4x} \sum_{v_k \in s_l} P(v_t = v_k). \end{aligned} \quad (27)$$

\mathbf{C} is the set of all contacts of the source user. $v_t = v_k$ implies that v_k is chosen as the destination user v_t after being selected as a contact. In other words,

$$P(v_t = v_k) = P(v_k \in \mathbf{C}) \cdot P(v_t = v_k | v_k \in \mathbf{C}). \quad (28)$$

Now we have the average number of hops in Eq. (29) by the integration of Eq. (26) - Eq. (28):

$$\begin{aligned} E[X] &= \sum_{q=1}^n P(k = q) \cdot \\ &\quad \sum_{x=1}^{\frac{1}{r(n)}} x \cdot \sum_{l=1}^{4x} \sum_{v_k \in s_l} P(v_k \in \mathbf{C}) \cdot P(v_t = v_k | v_k \in \mathbf{C}). \end{aligned} \quad (29)$$

The set $\{v_{i_1}, v_{i_2}, \dots, v_{i_q}\}$ contains q contacts of the source user. Taking all possible combinations into consideration, the probability that the source user has q contacts is

$$\begin{aligned} P(|\mathbf{C}| = q) &= \sum_{1 \leq i_1 \leq i_2 \leq \dots \leq i_q \leq N} P(\mathbf{C} = \{v_{i_1}, v_{i_2}, \dots, v_{i_q}\}) \\ &= \sum_{1 \leq i_1 \leq i_2 \leq \dots \leq i_q \leq N} \frac{(q^{-(\gamma-1)})^q \cdot q_{i_1}^{-\epsilon} q_{i_2}^{-\epsilon} \dots q_{i_q}^{-\epsilon}}{(M_{\gamma, \epsilon})^q}, \end{aligned}$$

where N is the number of users whose degree is less than q and the source user selects contacts only among these users. N grows as fast as n because

$$N = n \cdot \frac{\sum_{b=1}^{q-1} b^{-\gamma}}{\sum_{b=1}^n b^{-\gamma}} = \Theta(n).$$

The probability that \mathbf{C} consists of q particular users is

$$P(\mathbf{C} = \{v_{i_1}, v_{i_2}, \dots, v_{i_q}\}) = \frac{q_{i_1}^{-\epsilon} q_{i_2}^{-\epsilon} \dots q_{i_q}^{-\epsilon}}{\sum_{1 \leq i_1 \leq \dots \leq i_q \leq N} q_{i_1}^{-\epsilon} q_{i_2}^{-\epsilon} \dots q_{i_q}^{-\epsilon}}.$$

Consequently, the probability that v_k is chosen as a contact is given in Eq. (30) and simplified with the elementary symmetric polynomials in Definition 1 and 2:

$$P(v_k \in \mathbf{C}) = \frac{q_k^{-\epsilon} \cdot \sum_{1 \leq i_1 \leq \dots \leq i_{q-1} \leq N} q_{i_1}^{-\epsilon} q_{i_2}^{-\epsilon} \dots q_{i_{q-1}}^{-\epsilon}}{\sum_{1 \leq i_1 \leq \dots \leq i_q \leq N} q_{i_1}^{-\epsilon} q_{i_2}^{-\epsilon} \dots q_{i_q}^{-\epsilon}} \quad (30)$$

$$= \frac{q_k^{-\epsilon} \cdot \sigma_{q-1, N-1}^{\bar{k}}(Q)}{\sigma_{q, N}(Q)}.$$

Then we have Lemma 3 after expanding Eq. (29) with Eq. (30). ■

B. Proof of Lemma 4

A transformation of the Lemma 1 suggests that

$$\frac{\sigma_{1, N}(Q) \cdot \sigma_{q-1, N}(Q)}{q \cdot \sigma_{q, N}(Q)} = \Theta\left(\frac{N}{N-q+1}\right) = \Theta(1). \quad (31)$$

Moreover, the probability that the degree of the source user is not greater than q_0 is

$$P(q \leq q_0) = \sum_{q=1}^{q_0} \frac{q^{-\gamma}}{\sum_{b=1}^n b^{-\gamma}} = \Theta(1). \quad (32)$$

Therefore, the upper bound of E_1 according to Eq. (9) and Eq. (31) - Eq. (32) is

$$E_1 < \sum_{x=1}^{\frac{1}{r(n)}} x \sum_{l=1}^{4x} \sum_{v_k \in s_l} \frac{q_k^{-\epsilon} \cdot \sigma_{q-1, N}(Q)}{q \cdot \sigma_{q, N}(Q)} \quad (33)$$

$$\equiv \frac{q_k^{-\epsilon}}{\sigma_{1, N}(Q)} \sum_{x=1}^{\frac{1}{r(n)}} x \sum_{l=1}^{4x} \sum_{v_k \in s_l} 1,$$

where the symbol \equiv indicates the same order of magnitude on the two sides of an equation.

All the n users are distributed uniformly in the unit area, and the side length of each square is $C_1 r(n)$, so the summation term in Eq. (33) can be solved as

$$\sum_{x=1}^{\frac{1}{r(n)}} x \sum_{l=1}^{4x} \sum_{v_k \in s_l} 1 \equiv \sum_{x=1}^{\frac{1}{r(n)}} x \cdot 4x \cdot C_1^2 r^2(n) \cdot n \cdot 1 \quad (34)$$

$$\equiv n \cdot r(n)^2 \sum_{x=1}^{\frac{1}{r(n)}} x^2 \equiv \Theta\left(n \cdot r(n)^{-1}\right).$$

The $q_k^{-\epsilon}$ term in Eq. (33) can be replaced with its mean value in the upper bound for convenience:

$$E[q_k^{-\epsilon}] = \sum_{b=1}^{q-1} P(k=b) \cdot b^{-\epsilon} = \frac{\sum_{b=1}^{q-1} b^{-(\gamma+\epsilon)}}{\sum_{b=1}^n b^{-\gamma}} \equiv \Theta(1). \quad (35)$$

On the other hand,

$$\sigma_{1, N}(Q) = \sum_{j=1}^N q_j^{-\epsilon} \equiv N \cdot \int_1^{q-1} u^{-\epsilon} \frac{u^{-\gamma}}{\sum_{b=1}^n b^{-\gamma}} du \equiv \Theta(n). \quad (36)$$

By combining Eq. (33) - Eq. (36) together, the upper bound of E_1 is obtained:

$$E_1 = O\left(r(n)^{-1}\right). \quad (37)$$

Similarly, the lower bound of E_1 is

$$E_1 > \sum_1^{\frac{1}{r(n)}} x \sum_{l=1}^{4x} \sum_{v_k \in s_l} \frac{q_k^{-\epsilon} \cdot \sigma_{q-1, N}(Q) - q_k^{-2\epsilon} \cdot \sigma_{q-2, N}(Q)}{q \cdot \sigma_{q, N}(Q)}$$

$$= \text{upper bound} - \sum_1^{\frac{1}{r(n)}} x \sum_{l=1}^{4x} \sum_{v_k \in s_l} \frac{q_k^{-2\epsilon} \cdot \sigma_{q-2, N}(Q)}{q \cdot \sigma_{q, N}(Q)}.$$

It turns out that the second term in the lower bound is

$$\sum_{x=1}^{\frac{1}{r(n)}} x \sum_{l=1}^{4x} \sum_{v_k \in s_l} \frac{q_k^{-2\epsilon} \cdot \sigma_{q-2, N}(Q)}{q \cdot \sigma_{q, N}(Q)} \equiv \Theta\left(n^{-1} \cdot r(n)^{-1}\right). \quad (38)$$

The order in Eq. (38) is negligible compared with the upper bound in Eq. (37), so the order of E_1 in Eq. (10) is solved. ■

C. Proof of Lemma 5

Similar to the case E_1 , E_2 is given as

$$E_2 = \sum_{q=q_0+1}^n \frac{q^{-\gamma}}{\sum_{b=1}^n b^{-\gamma}} \cdot \sum_{x=1}^{\frac{1}{r(n)}} x \sum_{l=1}^{4x} \sum_{v_k \in s_l} \frac{q_k^{-\epsilon} \cdot \sigma_{q-1, N-1}^{\bar{k}}(Q)}{q \cdot \sigma_{q, N}(Q)}. \quad (39)$$

Since N is large enough and the degrees of q social contacts are independent and identically distributed, the law of large numbers can work here. Let $X_{i_j} = q_{i_j}^{-\epsilon}$, $Y_{i_j} = \log X_{i_j}$, and \bar{Y} denote the mean of Y_{i_j} , then we have

$$\frac{q_k^{-\epsilon} \cdot \sigma_{q-1, N-1}^{\bar{k}}(Q)}{q \cdot \sigma_{q, N}(Q)} \equiv \frac{\sum_{1 \leq i_1 \leq \dots \leq i_{q-1} \leq N, \exists m, i_m = k} \prod_{j=1}^{q-1} X_{i_j}}{q \cdot \sum_{1 \leq i_1 \leq \dots \leq i_q \leq N} \prod_{j=1}^q X_{i_j}}$$

$$\equiv \frac{\sum_{1 \leq i_1 \leq \dots \leq i_q \leq N, \exists m, i_m = k} \exp(\sum_{j=1}^q Y_{i_j})}{q \cdot \sum_{1 \leq i_1 \leq \dots \leq i_q \leq N} \exp(\sum_{j=1}^q Y_{i_j})}$$

$$\equiv \frac{\sum_{1 \leq i_1 \leq \dots \leq i_q \leq N, \exists m, i_m = k} \exp(q\bar{Y})}{q \cdot \sum_{1 \leq i_1 \leq \dots \leq i_q \leq N} \exp(q\bar{Y})}$$

$$\equiv \frac{\binom{N-1}{q-1}}{q \cdot \binom{N}{q}} = \frac{1}{N} = \Theta(n^{-1}). \quad (40)$$

Besides, the probability that the degree of the source user is greater than q_0 is

$$P(q > q_0) = \sum_{q=q_0+1}^n \frac{q^{-\gamma}}{\sum_{b=1}^n b^{-\gamma}} = \Theta(1). \quad (41)$$

Then Eq. (39) can be simplified by Eq. (40) - Eq. (41), namely:

$$E_2 \equiv \sum_{x=1}^{\frac{1}{r(n)}} x \sum_{l=1}^{4x} \sum_{v_k \in s_l} \frac{1}{n} \equiv \Theta\left(r(n)^{-1}\right). \quad (42)$$

Therefore, Lemma 5 is proven. ■

D. Proof of Theorem 3

Before giving the proof, the definition of moment generating function [65] and its properties need to be introduced.

Definition 3. For a discrete random variable X , its moment generating function is defined as:

$$\phi_X(t) = E[e^{tX}] = \sum_{x=0}^{\infty} e^{tx} \cdot P(X = x).$$

In addition, it is easy to obtain some useful properties of moment generating function:

Property 1 : $\phi_X(0) = \sum_{x=0}^{\infty} P(X = x) = 1$.

Property 2 : $\phi'_X(0) = E[X]$.

Property 3 : For the discrete random variables X, Y and Z , if $Z = X + Y$, and X and Y are independent of each other, then $\phi_Z(t) = \phi_X(t) \cdot \phi_Y(t)$.

Now, Theorem 3 can be proven.

In the first place, some symbols are defined: $M_\gamma = \sum_{k=1}^n k^{-\gamma}$ and $M_\epsilon = \sum_{k=1}^n k^{-\epsilon}$ are two normalization factors; $\bar{K}^{(L)}$ denotes the average degree of *level-L* ($L = 1, 2, \dots, L_{max}$); each social connection has two end users, and D stands for the degree of one end user when that of another end user is known. When the degree of Alice is known in Fig. 2(b), for example, the degree distribution of Bob follows the power-law $P(D = k) = \frac{k^{-\epsilon}}{M_\epsilon}$, $k = 1, 2, \dots, n$ according to $P(k_1, k_2)$; \bar{D} is the expectation of D .

Hereinafter the focus is the order of capacity. When n goes to positive infinity, some of their values can be calculated as below since γ and ϵ are both greater than 2:

$$M_\gamma = \sum_{k=1}^n k^{-\gamma} = \frac{k^{1-\gamma}}{\gamma-1} \Big|_n^1 \approx \frac{1}{\gamma-1},$$

$$M_\epsilon = \sum_{k=1}^n k^{-\epsilon} = \frac{k^{1-\epsilon}}{\epsilon-1} \Big|_n^1 \approx \frac{1}{\epsilon-1},$$

$$\bar{K}^{(1)} = E[K^{(1)}] = \sum_{k=1}^n k \cdot P(K^{(1)} = k) \approx \frac{\gamma-1}{\gamma-2},$$

$$\bar{D} = E[D] = \sum_{k=1}^n k \cdot P(D = k) = \sum_{k=1}^n k \cdot \frac{k^{-\epsilon}}{M_\epsilon} \approx \frac{\epsilon-1}{\epsilon-2}.$$

As depicted in Fig. 2(b), the *level-1* degree of Alice is known to be $K^{(1)}$, and we intend to solve the average *level-2* degree $K^{(2)}$ of Alice, which can be expressed as:

$$K^{(2)} = (D_1 - 1) + (D_2 - 1) + \dots + (D_{K^{(1)}} - 1),$$

where $D_1, D_2, \dots, D_{K^{(1)}}$ are independently and identically power-law distributed as $P(D_i = k) = P(D = k) = \frac{k^{-\epsilon}}{M_\epsilon}$, $i = 1, 2, \dots, K^{(1)}$, $k = 1, 2, \dots, n$. The return connection is subtracted from each of D_i to alleviate the impact of the loops. And $K^{(1)}$ follows the aforementioned power-law distribution $P(k)$, i.e., $P(K^{(1)} = k) = \frac{k^{-\gamma}}{M_\gamma}$, $k = 1, 2, \dots, n$.

Define $K'^{(2)} = \sum_{i=1}^{K^{(1)}} D_i$, then $K^{(2)} = K'^{(2)} - K^{(1)}$.

Under the condition of $K^{(1)}$, the moment generating function of $K'^{(2)}$ is written as:

$$\phi_{K'^{(2)}}(t) = E[e^{tK'^{(2)}}] = \sum_{k=1}^n P(K^{(1)} = k) \cdot E[e^{tK'^{(2)}} | K^{(1)} = k].$$

According to the Property 3 of moment generating function:

$$E[e^{tK'^{(2)}} | K^{(1)} = k] = \phi_{D_1}(t) \cdot \phi_{D_2}(t) \cdot \dots \cdot \phi_{D_k}(t) = [\phi_D(t)]^k.$$

Then $\phi_{K'^{(2)}}(t)$ is:

$$\phi_{K'^{(2)}}(t) = \sum_{k=1}^n P(K^{(1)} = k) \cdot [\phi_D(t)]^k.$$

Now calculate the expectation of $K'^{(2)}$ by the Property 1 and 2 of moment generating function:

$$\begin{aligned} E[K'^{(2)}] &= \phi'_{K'^{(2)}}(t)|_{t=0} \\ &= \sum_{k=1}^n k \cdot P(K^{(1)} = k) \cdot [\phi_D(t)]^{k-1} \cdot \phi'_D(t)|_{t=0} \\ &= \sum_{k=1}^n k \cdot P(K^{(1)} = k) \cdot 1^{k-1} \cdot \bar{D} \\ &= \bar{D} \cdot \bar{K}^{(1)}. \end{aligned}$$

Therefore, the average *level-2* degree $\bar{K}^{(2)}$ is

$$\bar{K}^{(2)} = E[K'^{(2)} - K^{(1)}] = (\bar{D} - 1) \cdot \bar{K}^{(1)} = \frac{1}{\epsilon-2} \cdot \frac{\gamma-1}{\gamma-2}.$$

When $L \geq 3$, the average *level-L* degree can be derived in the same way. The *level-L* degree $K^{(L)}$ can be expanded as:

$$K^{(L)} = (D_1 - 1) + (D_2 - 1) + \dots + (D_{K^{(L-1)}} - 1) = K'^{(L)} - K^{(L-1)},$$

where the variables $D_1, D_2, \dots, D_{K^{(L-1)}}$ are independently and identically distributed as $P(D = k)$, and $K'^{(L)} = \sum_{i=1}^{K^{(L-1)}} D_i$.

The moment generating function of $K'^{(L)}$ is:

$$\begin{aligned} \phi_{K'^{(L)}}(t) &= E[e^{tK'^{(L)}}] \\ &= \sum_{k=1}^n P(K^{(L-1)} = k) \cdot E[e^{tK'^{(L)}} | K^{(L-1)} = k], \end{aligned}$$

and the expectation of $K'^{(L)}$ can be solved as:

$$\begin{aligned} E[K'^{(L)}] &= \phi'_{K'^{(L)}}(t)|_{t=0} \\ &= \sum_{k=1}^n k \cdot P(K^{(L-1)} = k) \cdot [\phi_D(t)]^{k-1} \cdot \phi'_D(t)|_{t=0} \\ &= \sum_{k=1}^n k \cdot P(K^{(L-1)} = k) \cdot 1^{k-1} \cdot \bar{D} \\ &= \bar{D} \cdot \bar{K}^{(L-1)}. \end{aligned}$$

That is to say, the average *level-L* degree can be written as:

$$\begin{aligned} \bar{K}^{(L)} &= E[K'^{(L)} - K^{(L-1)}] \\ &= (\bar{D} - 1) \cdot \bar{K}^{(L-1)} \\ &= \frac{1}{\epsilon-2} \cdot \bar{K}^{(L-1)}. \end{aligned}$$

Therefore, the final expression of $\overline{K}^{(L)}$ in Eq. (17) is obtained:

$$\overline{K}^{(L)} = \left(\frac{1}{\epsilon - 2} \right)^{L-1} \cdot \frac{\gamma - 1}{\gamma - 2}, \quad L = 1, 2, \dots, L_{\max}.$$

REFERENCES

- [1] Z. Wang, L. Sun, M. Zhang, H. Pang, E. Tian, and W. Zhu, "Propagation- and mobility-aware D2D social content replication," *IEEE Trans. on Mobile Comput.*, vol. 16, no. 4, pp. 1107–1120, 2017.
- [2] J. Guo, J. Ma, X. Li, T. Zhang, and Z. Liu, "A situational awareness trust evolution model for mobile devices in D2D communication," *IEEE Access*, vol. 6, no. 99, pp. 4375–4386, Sep. 2017.
- [3] 3GPP TS 22.278, Section 7A, "Service requirements for the evolved packet system (EPS)," Dec. 2015.
- [4] D. Wu, L. Zhou, and Y. Cai, "Social-aware rate based content sharing mode selection for D2D content sharing scenarios," *IEEE Trans. on Multimedia*, vol. 19, no. 11, pp. 2571–2582, 2017.
- [5] P. Jacquet, "Capacity of simple multiple-input-single-output wireless networks over uniform or fractal maps," *IEEE 21st International Symposium on Modeling, Analysis and Simulation of Computer and Telecommunication Systems (MASCOTS)*, pp. 444–453, Aug. 2013.
- [6] —, "Optimized outage capacity in random wireless networks in uniform and fractal maps," *IEEE International Symposium on Information Theory (ISIT)*, Hong Kong, China, Jun. 2015.
- [7] T. Maksymyuk, M. Brych, I. Strykhalyuk, and M. Jo, "Fractal modeling for multi-tier heterogeneous networks with ultra-high capacity demands," *Smart Comput. Rev.*, vol. 5, no. 4, pp. 346–355, Aug. 2015.
- [8] C. C. Chen, J. S. Daponte, and M. D. Fox, "Fractal feature analysis and classification in medical imaging," *IEEE Trans. Med. Imag.*, vol. 8, no. 2, pp. 133–142, Jan. 1989.
- [9] B. B. Mandelbrot and J. A. Wheeler, "The fractal geometry of nature," *J. R. Stat. Soc.*, vol. 147, no. 4, pp. 468–476, Jun. 1983.
- [10] K. J. Falconer, "Fractal geometry-mathematical foundations and applications," *Biometrics*, vol. 46, no. 3, pp. 499–510, Nov. 2003.
- [11] L. K. Gallos, C. Song, and H. A. Makse, "Scaling of degree correlations and its influence on diffusion in scale-free networks," *Phys. Rev. Lett.*, vol. 100, no. 24, pp. 248–701, Jun. 2008.
- [12] C. Song, S. Havlin, and H. A. Makse, "Origins of fractality in the growth of complex networks," *Nature Phys.*, vol. 2, no. 4, pp. 275–281, Mar. 2006.
- [13] C. Song, L. K. Gallos, S. Havlin, and H. A. Makse, "How to calculate the fractal dimension of a complex network: the box covering algorithm," *J. Stat. Mech-Theory E.*, vol. 2007, no. 3, pp. 297–316, Jan. 2007.
- [14] C. Song, S. Havlin, and H. A. Makse, "Self-similarity of complex networks," *Nature*, vol. 433, no. 7024, pp. 392–406, Jan. 2005.
- [15] R. Albert and A. Barabasi, "Statistical mechanics of complex networks," *Rev. Mod. Phys.*, vol. 74, no. 1, Jan. 2002.
- [16] M. E. J. Newman, "The structure and function of complex networks," *SIAM Rev.*, vol. 45, no. 2, pp. 167–256, Jun. 2003.
- [17] R. Albert and H. Jeong, "Internet: diameter of the world-wide web," *Nature*, vol. 401, no. 6, pp. 130–131, Sep. 1999.
- [18] M. Faloutsos, P. Faloutsos, and C. Faloutsos, "On power-law relationships of the internet topology," *SIGCOMM'99*, vol. 29, no. 4, pp. 251–262, Sep. 1999.
- [19] C. Yuan, Z. Zhao, R. Li, M. Li, and H. Zhang, "Not call me cellular any more: the emergence of scaling law, fractal patterns and small-world in wireless networks," *IEEE Access*, vol. 5, no. 1, pp. 3132–3130, Mar. 2017.
- [20] P. Gupta and P. R. Kumar, "The capacity of wireless networks," *IEEE Trans. Information Theory*, vol. 46, no. 2, pp. 388–404, Mar. 2000.
- [21] M. Gastpar and M. Vetterli, "On the capacity of wireless networks: The relay case," *Proc. IEEE INFOCOM 2002*, New York, NY, USA, Jun. 2002.
- [22] B. Azimdoost, H. R. Sadjadpour, and J. J. Garcia-luna-aceves, "On the capacity of hybrid wireless networks," *Eurasip J. Wireless Commun. and Netw.*, vol. 2010, no. 1, pp. 1–9, Sep. 2009.
- [23] M. Karimzadeh Kiskani, B. Azimdoost, and H. R. Sadjadpour, "Effect of social groups on the capacity of wireless networks," *IEEE Trans. Wireless Commun.*, vol. 15, no. 1, pp. 3–13, Jan. 2016.
- [24] N. Michele, A. S. George, P. Vlad, and F. Mauro, "When social networks meet D2D communications: A survey," *Sensors*, vol. 19, no. 2, pp. 396–411, Jan. 2019.
- [25] A. Ometov, A. Orsino, L. Militano, et al., "A novel security-centric framework for D2D connectivity based on spatial and social proximity," *Computer Networks*, vol. 107, no. 2, pp. 327–338, Apr. 2016.
- [26] X. Chen, B. Proulx, X. Gong, et al., "Exploiting social ties for cooperative D2D communications: a mobile social networking case," *IEEE/ACM Trans. on Networking*, vol. 23, no. 5, pp. 1471–1484, Oct. 2015.
- [27] Y. Li, T. Wu, P. Hui, et al., "Social-aware D2D communications: qualitative insights and quantitative analysis," *IEEE Communications Magazine*, vol. 52, no. 6, pp. 150–158, Jun. 2014.
- [28] A. Ometov, A. Orsino, L. Militano, et al., "Toward trusted, social-aware D2D connectivity: bridging across the technology and sociality realms," *IEEE Wireless Communications*, vol. 23, no. 4, pp. 103–111, Aug. 2016.
- [29] J. P. Friesen, A. C. Kay, R. P. Eibach, et al., "Seeking structure in social organization: compensatory control and the psychological advantages of hierarchy," *Journal of Personality and Social Psychology*, vol. 106, no. 4, pp. 590–609, Feb. 2014.
- [30] Fei Hao and Hai Wang, "TFRank: an evaluation of users importance with fractal views in social networks," *Waset Org*, 2013.
- [31] V. De Florio and M. Bakhouya, "Mutualistic relationships in service-oriented communities and fractal social organizations," *Complex Systems (WCCS), 2014 Second World Conference*, Agadir, Morocco, Nov. 2014.
- [32] Y. J. Chun, G. B. Colombo, S. L. Cotton, W. G. Scanlon, R. M. Whittaker, and S. Allen, "Device-to-device communications: a performance analysis in the context of social comparison based relaying," *IEEE Trans. on Wireless Commun.*, vol. 16, no. 12, pp. 7733–7745, Dec. 2017.
- [33] L. Wang, Z. Li, M. Chen, A. Zhang, J. W. Cui, and B. Zheng, "Secure content sharing protocol for D2D users based on profile matching in social networks," *International Conference on Wireless Communications and Signal Processing (WCSP)*, Nanjing, China, Oct. 2017.
- [34] L. Militano, A. Orsino, G. Araniti, and et al., "Trust-based and social-aware coalition formation game for multihop data uploading in 5G systems," *Computer Networks*, Sep. 2016.
- [35] M. Garetto, P. Giaccone, and E. Leonardi, "Capacity scaling in delay tolerant networks with heterogeneous mobile nodes," *Proceedings of the 8th ACM International Symposium on Mobile Ad hoc Networking and Computing*, Montreal, Quebec, Canada, Sep. 2007.
- [36] S. Qin, G. Feng, and Y. Zhang, "How the contact-probing mechanism affects the transmission capacity of delay-tolerant networks," *IEEE Trans. Vehicular Technology*, vol. 60, no. 4, pp. 1825–1834, Mar. 2011.
- [37] Emad Abd-Elrahman, H. Afifi, L. Atzori, et al., "IoT-D2D task allocation: an award-driven game theory approach," *2016 23rd International Conference on Telecommunications (ICT)*, Thessaloniki, Greece, May. 2016.
- [38] D. Kozio, F. S. Moya, L. Yu, et al., "QoS and service continuity in 3GPP D2D for IoT and wearables," *2017 IEEE Conference on Standards for Communications and Networking (CSCN)*, Helsinki, Finland, Sep. 2017.
- [39] X. Chen, J. Shen, J. Wu, "A novel information model for efficient routing protocols in delay tolerant networks," *IEEE International Symposium on Parallel & Distributed Processing*, Jun. 2017.
- [40] T. Spyropoulos, K. Psounis, and C. S. Raghavendra, "Spray and wait: an efficient routing scheme for intermittently connected mobile networks," *Proceedings of the 2005 ACM SIGCOMM workshop on Delay-tolerant networking*, Philadelphia, Pennsylvania, USA, Aug. 2005.
- [41] A. Lindgren, A. Doria, and O. Schelen, "Probabilistic routing in intermittently connected networks," *SIGMOBILE Mob. Comput. Commun. Rev.*, vol. 7, no. 3, pp. 19–27, Nov. 2003.
- [42] J. Leguay, T. Friedman, and V. Conan, "Evaluating mobility pattern space routing for DTNs," *Proceedings of the 25th IEEE International Conference on Computer Communications (INFOCOM)*, Barcelona, Spain, Apr. 2006.
- [43] C. Liu and J. Wu, "Scalable routing in delay tolerant networks," *Proceedings of the 8th ACM international symposium on Mobile ad hoc networking and computing*, Montreal, Quebec, Canada, Sep. 2007.
- [44] —, "An optimal probabilistic forwarding protocol in delay tolerant networks," *Proceedings of the 10th ACM international symposium on Mobile ad hoc networking and computing*, New Orleans, LA, USA, May. 2009.
- [45] R. Urgaonkar and M. J. Neely, "Network capacity region and minimum energy function for a delay-tolerant, mobile ad hoc network," *IEEE/ACM Trans. Networking*, vol. 19, no. 4, pp. 1137–1150, Jan. 2011.
- [46] S. R. Kulkarni and P. Viswanath, "A deterministic approach to throughput scaling in wireless networks," *IEEE Trans. Information Theory*, vol. 50, no. 50, pp. 351–366, Jul. 2002.
- [47] B. Azimdoost, H. R. Sadjadpour, and J. J. Garcia-Luna-Aceves, "The impact of social groups on the capacity of wireless networks," *Netw. Sci. Workshop*, West Point, NY, USA, Jun. 2011.

- [48] M. K. Kiskani, H. Sadjadpour, and M. Guizani, "Social interaction increases capacity of wireless networks," *Wireless Commun. Mobile Comput. Conf.*, Sardinia, Italy, Jul. 2013.
- [49] B. Azimdoost and H. R. Sadjadpour, "Capacity of scale free wireless networks," *2012 IEEE Global Communications Conference (GLOBECOM)*, Anaheim, CA, USA, Apr. 2013.
- [50] B. Azimdoost, C. Westphal, and H. R. Sadjadpour, "Fundamental limits on throughput capacity in information-centric networks," *IEEE Trans. Commun.*, vol. 64, no. 12, pp. 5037–5049, Oct. 2016.
- [51] X. Ge, Y. Qiu, and et al., "Wireless fractal cellular networks," *IEEE Wireless Commun.*, vol. 23, no. 5, pp. 110–119, Oct. 2016.
- [52] Y. Hao, M. Chen, L. Hu, J. Song, M. Volk, and I. Humar, "Wireless fractal ultra-dense cellular networks," *Sensors*, vol. 17, no. 4, Apr. 2017.
- [53] S. H. Strogatz, "Complex systems: romanesque networks," *Nature*, vol. 433, no. 7024, pp. 365–376, Jan. 2005.
- [54] A. Kaur and R. Khanna, "A stacked Sierpinski gasket fractal microstrip antenna for IEEE802.11a/b/UNII-1 and C band applications," *2015 IEEE 4th Asia-Pacific Conference on Antennas and Propagation (APCAP)*, Kuta, Indonesia, Jul. 2016.
- [55] S. S. Haider, M. R. Wali, F. A. Tahir, and M. U. Khan, "A fractal dual-band polarization diversity antenna for 5G applications," *2017 IEEE International Symposium on Antennas and Propagation and USNC/URSI National Radio Science Meeting*, San Diego, CA, USA, Jul. 2017.
- [56] X. Cai, J. Zheng, Z. Yuan, and H. Murata, "A capacity oriented resource allocation algorithm for device-to-device communication in mobile cellular networks," *2014 IEEE International Conference on Communications (ICC)*, Sydney, NSW, Australia, Jun. 2014.
- [57] W. Min, X. Wang, X. Chai, and H. Wei, "The impact of device-to-device communication on the capacity of cellular systems," *2016 International Conference on Computer, Information and Telecommunication Systems (CITS)*, Kunming, China, Jul. 2016.
- [58] Y. S. Liou, R. H. Gau, and C. J. Chang, "Group partition and dynamic rate adaptation for scalable capacity-region-aware device-to-device communications," *IEEE Trans. Wireless Communications*, vol. 14, no. 2, pp. 921–934, Feb. 2015.
- [59] R. Cohen and S. Havlin, "Scale-free networks are ultrasmall," *Phys. Rev. Lett.*, vol. 90, no. 5, pp. 658–671, Feb. 2003.
- [60] X. Feng and P. R. Kumar, "Scaling laws for ad hoc wireless networks: an information theoretic approach," *Foundations and Trends in Networking*, vol. 1, no. 2, pp. 16–47, Jan. 2006.
- [61] M. D. Penrose, "The longest edge of the random minimal spanning tree," *Ann. Appl. Probab.*, vol. 7, no. 2, pp. 222–230, 1996.
- [62] B. Latane and A. Others, "Distance matters: physical space and social impact," *PSPB*, vol. 21, no. 8, pp. 795–805, Aug. 1995.
- [63] T. P. Mitev, "New inequalities between elementary symmetric polynomials," *Journal of Inequalities in Pure and Applied Mathematics (JIPAM)*, vol. 4, no. 2, pp. 48–56, 2003.
- [64] P. Mahadevan, D. Krioukov, K. Fall, and A. Vahdat, "Systematic topology analysis and generation using degree correlations," *ACM SIGCOMM Comput. Commun. Rev.*, Pisa, Italy, Jun. 2006.
- [65] S. H. Simon, A. L. Moustakas, and L. Marinelli, "Capacity and character expansions: moment-generating function and other exact results for MIMO correlated channels," *IEEE Trans. on Information Theory*, vol. 52, no. 12, pp. 5336–5351, 2006.